scientific reports

Check for updates

OPEN

Identification and validation of palmitoylation-related biomarkers in gestational diabetes mellitus

Kai Zhang[1,4], Xiaoyang Shi[2,4], Rongrong Bian[1], Wei Shi[3], Li Yang[3] & Chenchen Ren[3]✉

Palmitoylation plays a crucial role in the pathophysiology of diabetes, and an increase in palmitoylation may inhibit the function of insulin receptors, thereby affecting the progression of gestational diabetes mellitus (GDM). However, its involvement in gestational diabetes mellitus (GDM) remains underexplored. This study analyzed GDM-related datasets and 30 palmitoylation-related genes (PRGs), identifying MNDA, FCGR3B, and AQP9 as significantly upregulated biomarkers in GDM samples. Consistent with the dataset analysis, reverse transcription-polymerase chain reaction (RT-qPCR) confirmed elevated AQP9 expression. Comprehensive analyses, including nomogram construction, enrichment analysis, immune infiltration assessment, molecular regulatory network generation, drug prediction, and molecular docking, were conducted. The biomarker-based nomogram demonstrated excellent predictive performance for GDM risk. MNDA, FCGR3B, and AQP9 were significantly enriched in pathways such as "Myc-targets-v1" and "TNFA signaling *via* NFkB." Additionally, eosinophil infiltration showed a strong positive correlation with these biomarkers. Regulatory networks involving SH3BP5-AS1-hsa-miR-182-5p-AQP9 and hsa-miR-182-5p-AQP9-ELF5 were identified, and stable binding energies were observed between the biomarkers and corresponding drugs. These findings provide promising avenues for early GDM screening and diagnosis.

Keywords Palmitoylation, Gestational diabetes mellitus, Diagnosis, MNDA, FCGR3B, AQP9

Abbreviations

GDM	Gestational diabetes mellitus
PRGs	Palmitoylation related genes
DEGs	Differentially expressed genes
PPI	Protein-protein interaction
RT-qPCR	Reverse transcription quantitative polymerase chain reaction
T2DM	Type 2 diabetes mellitus
GLUT4	Glucose transporter 4
ssGSEA	Single-sample gene set enrichment analysis
BP	Biological process
CC	Cellular component
MF	Molecular function
MSigDB	Molecular signatures database
miRNAs	MicroRNAs
lncRNAs	Long non-coding RNAs
TFs	Transcription factors
SNPs	Single nucleotide polymorphisms
PDB	Protein data bank
MNDA	Myeloid nuclear differentiation antigen
FCGRs	FCGR genes in immune effector cells express fc-gamma receptors
CNVs	Copy number variants

[1]Department of General Medicine, Department of Intensive Care Unit, The Third Affiliated Hospital of Zhengzhou University and Henan Province Women and Children's Hospital, Zhengzhou 450052, Henan, P.R. China. [2]Department of Endocrinology, People's Hospital of Zhengzhou University, Henan Provincial People's Hospital, Henan Provincial Key Laboratory of Intestinal Microecology and Diabetes Control, Zhengzhou 450003, Henan, P.R. China. [3]Department of Obstetrics and Gynecology, The Third Affiliated Hospital of Zhengzhou University and Henan Province Women and Children's Hospital, Zhengzhou 450052, Henan, P.R. China. [4]These authors contributed equally: Kai Zhang and Xiaoyang Shi. ✉email: renchenchen1106@126.com

AQPs	Aquaporins
FCGR3B	Fc Gamma Receptor IIIb
AQP9	Aquaporin 9
TNFA	Tumor Necrosis Factor
GEO	Gene Expression Omnibus
TYROBP	Transmembrane Immune Signaling Adaptor TYROBP
BST2	Bone Marrow Stromal Cell Antigen 2
S100A6	S100 Calcium Binding Protein A6
KEGG	Kyoto Encyclopedia of Genes and Genomes
CXCL10	C-X-C Motif Chemokine Ligand 10
IFIT2	Interferon Induced Protein With Tetratricopeptide Repeats 2
GSVA	Gene Set Variation Analysis
GSEA	Gene Set Enrichment Analysis
NLRP3	NLR Family Pyrin Domain Containing 3
E2F1	E2F Transcription Factor 1
CDC422	Cell Division Control Protein 42
MALAT1	Metastasis Associated Lung Adenocarcinoma Transcript 1
MEG3	Maternally Expressed 3
PVT1	Pvt1 Oncogene
lnc-FFLs	LncRNA-associated feedforward loops
SH3BP5-AS1	SH3BP5 Antisense RNA 1
GO	Gene Ontology
STRING	Search Tool for the Retrieval of Interacting Genes/Proteins
BioGPS	Biomarkers into biology gene portal services
FDR	False discovery rate
NES	Normalized enrichment score

Gestational diabetes mellitus (GDM), a common metabolic complication of pregnancy, is defined as a form of diabetes that develops or is first diagnosed during pregnancy, characterized by hyperglycemia that typically resolves after the birth of the child[1,2]. Affecting up to 30% of pregnancies globally, depending on demographic factors, screening methods, and diagnostic criteria[3,4], GDM poses a significant public health challenge. It heightens the risk of severe prenatal complications and adverse birth outcomes for both mothers and infants. Women with GDM face an increased likelihood of developing impaired glucose tolerance and type 2 diabetes mellitus (T2DM) later in life, while their offspring are predisposed to obesity, insulin resistance, and T2DM[5,6]. Thus, comprehensive screening and early intervention are essential to mitigate these risks.

Palmitoylation, a reversible post-translational modification, regulates protein functions such as cell signaling, localization, trafficking, and protein-protein interactions[7]. Dynamic palmitoylation is regulated by a family of ZDHHC palmitoylating enzymes and some de-palmitoylating enzymes, and this modification plays a critical role in the pathogenesis of metabolic disorders, inflammatory diseases, neurodegeneration, and cancer[8–10]. Du et al. found that inactivation of palmitoyl acyltransferase in adipose tissue and muscle can suppress the membrane translocation of insulin-dependent glucose transporter 4 (GLUT4) and cause hyperglycemia. Recent research suggests that protein palmitoylation in islets can regulate glucose-stimulated insulin secretion and couple insulin hypersecretion with β cell failure in diabetes[11,12]. A recent UK study identified that a palmitoylated metabolite in maternal serum from 12 to 20 weeks of gestational age may be effective in the prediction of GDM at 28 weeks of gestational age[13]. According to research, palmitoyl modification in placental tissues also plays a role in maternal-fetal health. The placental mRNA levels of carnitine palmitoyl transferase-1 were lower in the preeclampsia group compared to the normotensive control group, which was associated with preterm birth[14]. The expression of placental carnitine palmitoyl-transferase-1B(CPT1B) was lower in older and overweight pregnant women, which may underlie decreased placental metabolic flexibility and potentially contribute to pregnancy complications[15]. Palmitoylation could exacerbate insulin resistance by inhibiting insulin receptor function and interfering with insulin signaling[16]. Moreover, Wang et al. found that astragaloside IV could upregulate insulin sensitivity by restoring CPT1A activity[17]. These investigations highlight a significant link between Palmitoylation and GDM. Hence, further understanding of molecular mechanisms of palmitoylation affecting GDM is crucial for exploring its underlying mechanism and new treatment options. However, research on palmitoylation-related biomarkers in GDM remains scarce, underscoring the need to identify novel biomarkers to elucidate the molecular mechanisms underlying the role of palmitoylation in GDM pathogenesis. Building on this, an in-depth analysis of the specific regulatory roles that the SNP-miRNA-mRNA signaling pathway may play helps reveal the intrinsic connection between biomarkers and the progression of GDM[7,18,19], offering new perspectives for the development of personalized treatments for GDM.

Using GDM transcriptome data from the Gene Expression Omnibus (GEO) database, this study employed bioinformatics approaches to identify palmitoylation-related biomarkers and validated the findings through reverse transcription-quantitative polymerase chain reaction (RT-qPCR). In addition, it may contribute to understanding the potential regulatory mechanisms between biomarkers and GDM progression by predicting miRNAs, lncRNAs and SNPs that target the biomarkers. Additional analyses, including enrichment analysis, immune infiltration profiling, drug sensitivity prediction, and molecular docking, offer valuable insights into the potential mechanisms of these biomarkers, paving the way for improved diagnostic and therapeutic strategies for GDM.

Results

Analysis of gene expression pattern differences in different datasets

In order to identify genes related to palmitoylation in GDM, the ssGSEA algorithm was used to calculate the scores of PRGs in each sample of the GSE203346 dataset. Based on the median PRG score, samples with scores greater than 6.176676 were classified into the high-score group, while those with scores lower than 6.176676 were classified into the low-score group. Then, we further explored the differentially expressed genes between these two groups. In the GSE203346 dataset, the box plot analysis revealed significant differences between groups stratified by the median PRG scores ($P < 0.05$), which is consistent with the cross-validation results (Supplementary Figure S1), indicating a potential association between palmitoylation and GDM progression (Fig. 1a). Differential expression analysis identified 1,260 DEGs1, comprising 1,022 upregulated and 238 downregulated genes (Fig. 1b-c). Additionally, 445 DEGs2 were identified in the comparison between GDM and control samples, including 272 upregulated and 173 downregulated genes (Fig. 1d-e).

Construction of the protein-protein interaction (PPI) network and identification of candidate genes

To identify genes closely related to GDM, the protein-protein interaction relationships and functional associations between the genes were further analyzed based on DEGs1 and DEGs2. The intersection of DEGs1 and DEGs2 yielded 105 shared genes (Fig. 2a). Correlation analysis revealed significant positive correlations among many intersection genes, including TYROBP, AQP9, BST2, and S100A6 ($|cor| > 0.3$, $P < 0.05$). The top 10 genes with the strongest positive and negative correlations were visualized in a heatmap (Fig. 2b). Enrichment analysis indicated that these genes were significantly associated with GO biological processes such as "defense response to symbiont and virus," "positive regulation of response to external stimuli," and "cytokine-cytokine receptor interaction" (Fig. 2c). KEGG pathway analysis further highlighted enrichments in pathways such as the "NOD-like receptor signaling pathway" and the "Cytosolic DNA-sensing pathway" (Fig. 2d). A PPI network was constructed, comprising 47 nodes and 102 edges, showcasing interactions among genes such as FCGR3B, AQP9, CXCL10, and IFIT2 (Fig. 2e). Using the Degree algorithm, 22 candidate genes were identified, with three additional genes ranked 20th included due to identical scores (Fig. 2f).

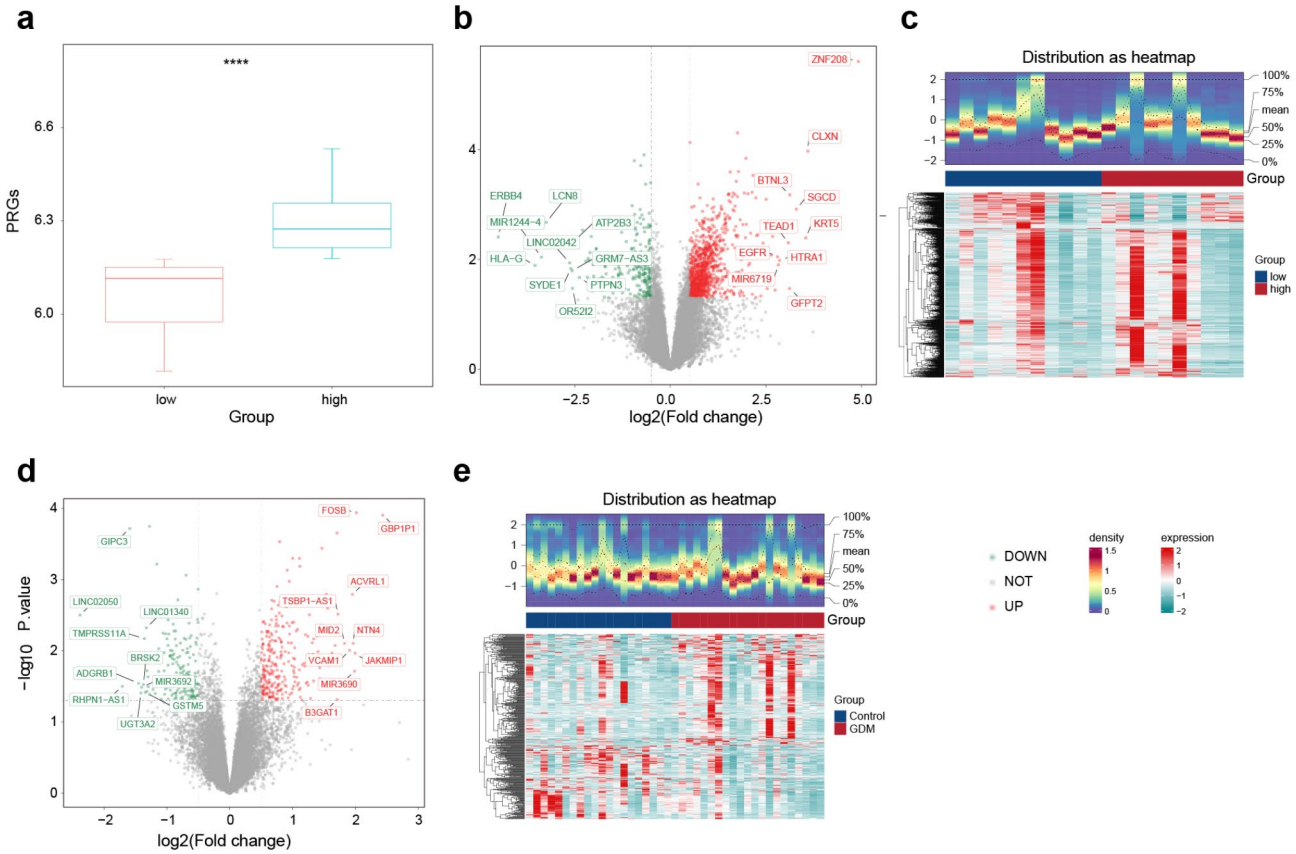

Fig. 1. Differential expression analysis for genes associated with palmitoylation in GDM. **(a)** PRG scores of the high and low score groups based on the median value in GDM ($P < 0.05$). **(b)** Volcano plot showing 1,260 DEGs1 between the high- and low-PRG score groups in GDM. **(c)** Heatmap of DEGs1 between the high- and low-PRG score groups. **(d)** Volcano plot showing 445 DEGs2 between GDM and controls. **(e)** Heatmap of DEGs2 between GDM and controls. PRGs, palmitoylation-related genes; GDM, gestational diabetes mellitus; DEGs, differentially expressed genes.

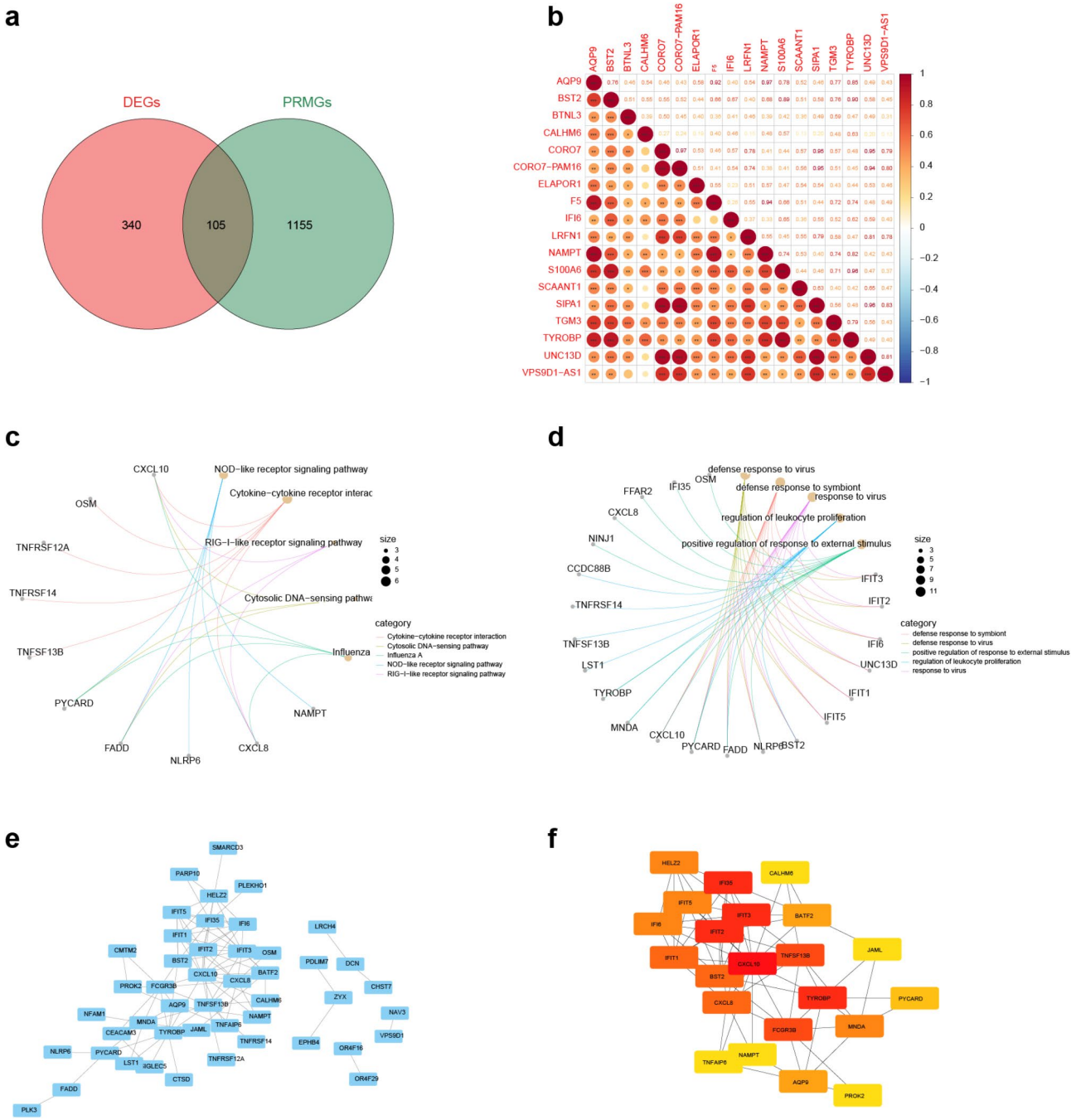

Fig. 2. Screening of candidate genes and analysis of functional enrichment. **(a)** Venn diagram showing 105 intersection genes by crossing DEGs1 and DEGs2. **(b)** Correlation heatmap of the top 10 intersection genes exhibiting the highest positive and negative correlations. **(c)** GO pathway-gene network diagram of intersection genes. **(d)** KEGG pathway-gene network diagram of intersection genes. **(e)** PPI network of the intersection genes. **(f)** Top 20 candidate genes identified by the Degree algorithm (including 3 genes ranked 20th with identical degrees). DEGs, differentially expressed genes; PPI, protein-protein interaction; GO, Gene Ontology; KEGG, Kyoto Encyclopedia of Genes and Genomes.

Analysis of the distribution patterns of biomarkers in chromosomes and subcellular compartments

Based on 22 candidate genes, biomarkers associated with the progression of GDM were identified through machine learning and expression validation. Further screening of the candidate genes using the xgboost and randomForest algorithms identified 16 and 7 feature genes, respectively (Fig. 3a-b). The intersection of these two sets yielded 7 candidate biomarkers (Fig. 3c). Among these genes, only MNDA, FCGR3B, and AQP9 exhibited consistent expression patterns in both the GSE203346 and GSE154414 datasets, and were significantly

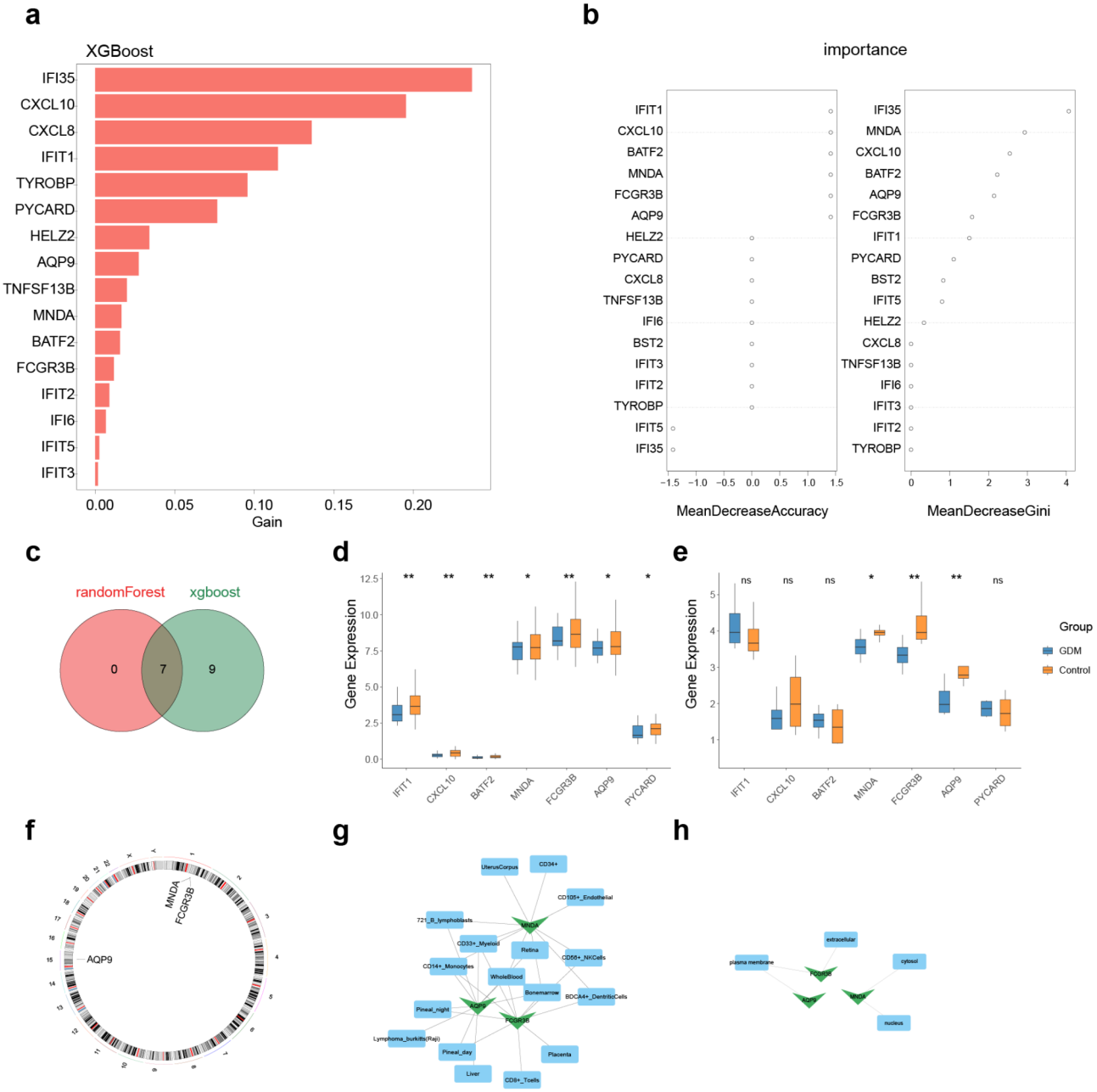

Fig. 3. Identification of biomarkers for GDM. **(a)** Histogram of 16 genes obtained using the XGBoost algorithm. **(b)** Genes identified by the Random Forest algorithm. **(c)** Venn diagram showing 7 candidate biomarkers by crossing the results of both machine learning algorithms. **(d-e)** Expression of the 7 candidate biomarkers between the GDM and control groups in both the GSE203346 **(d)** and GSE154414 **(e)** datasets (*$P<0.05$, **$P<0.01$, and ns; $P>0.05$). **(f)** Chromosomal localization of biomarkers. **(g)** Network map of the top 10 tissues/organs with the highest expression of biomarkers identified by BioGPS. **(h)** Network maps of the subcellular distribution of biomarkers.

upregulated in the GDM group compared to the control group ($P<0.05$). Therefore, MNDA, FCGR3B, and AQP9 were validated as biomarkers for GDM (Fig. 3d-e). Chromosomal and subcellular localization, as well as tissue expression, were then analyzed to examine the differences in the biomarkers across chromosomes, cells, and tissues, to further explore their expression patterns. Chromosomal localization analysis revealed that MNDA and FCGR3B are located on chromosome 1, while AQP9 is on chromosome 15 (Fig. 3f). Tissue distribution analysis indicated that these biomarkers are present in various tissues and organs, including bone marrow, CD14 + monocytes, and CD33 + myeloid whole blood (Fig. 3g). Subcellular localization analysis showed distinct patterns: FCGR3B and AQP9 were localized to the plasma membrane, while MNDA was found in the nucleus and cytosol (Fig. 3h).

Construction of the nomogram model and validation of its predictive performance

To explore the predictive ability of biomarkers for the occurrence of GDM, a nomogram model was constructed based on MNDA, FCGR3B, and AQP9 (Fig. 4a). The calibration curve validated the model's predictive accuracy (Fig. 4b), while the decision curve analysis indicated a positive net benefit, confirming its strong clinical utility for GDM assessment (Fig. 4c).

Enrichment pathway of MNDA, FCGR3B, and AQP9

Pathway enrichment analysis provided further insights into biomarker-related mechanisms. GSVA revealed that high-score groups for MNDA, FCGR3B, and AQP9 were enriched in pathways such as "spliceosome," "RNA degradation," and "NOD-like receptor signaling pathway." In contrast, low-score groups exhibited enrichment in "ECM-receptor interaction," "tyrosine metabolism," and "regulation of autophagy" (Supplementary Figure S2a-c). GSEA analysis indicated significant co-enrichment of these biomarkers in pathways including "Myc-targets-v1," "TNFα signaling *via* NFkB," "interferon γ response," and "interferon α response" (Supplementary Figure S1d-f). These results suggest that MNDA, FCGR3B, and AQP9 may influence GDM progression by modulating cellular proliferation, metabolism, inflammatory responses, and immune-related pathways.

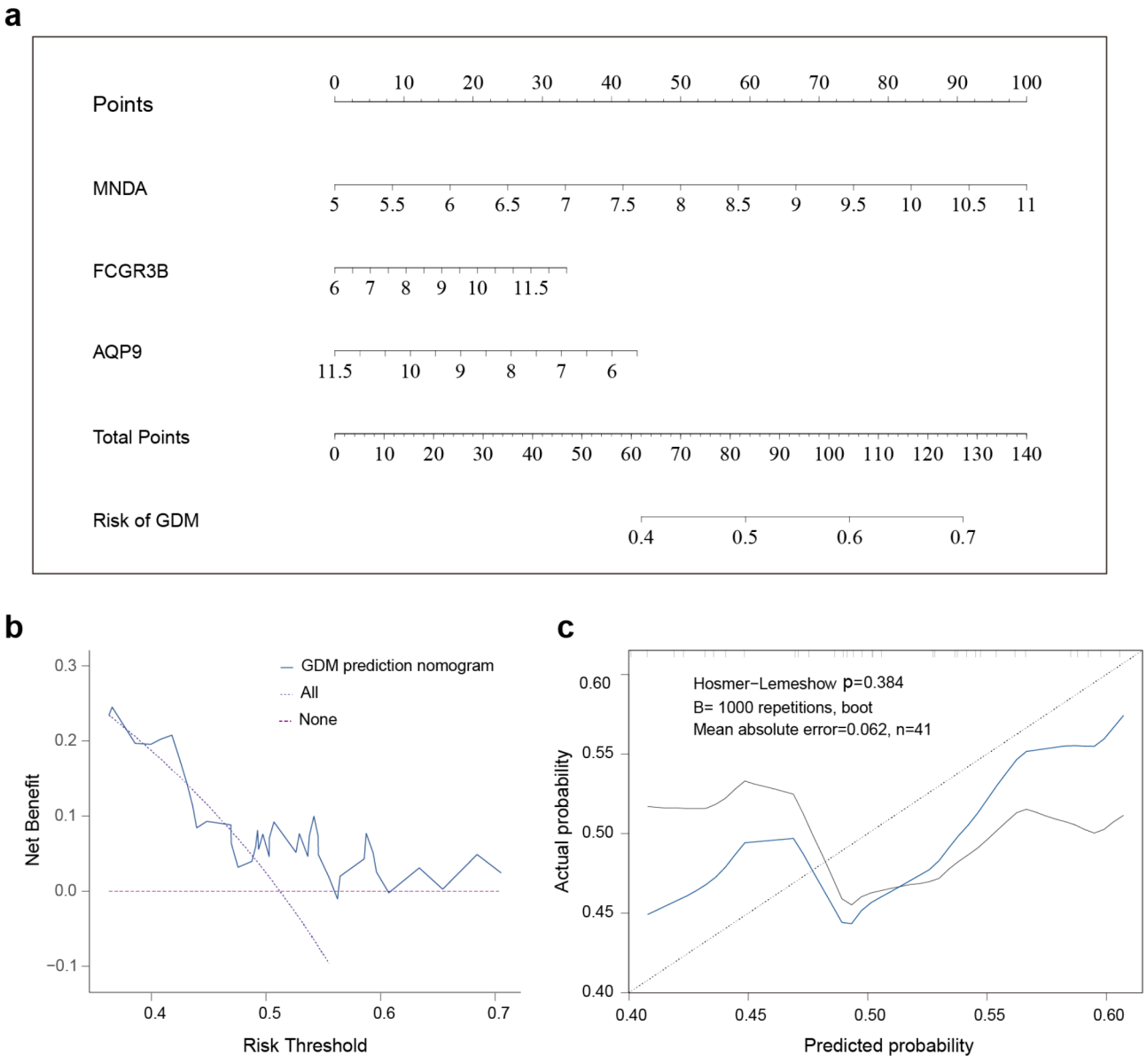

Fig. 4. Nomogram model construction for GDM prediction. **(a)** Nomogram based on the expression levels of MNDA, FCGR3B, and AQP9 to predict GDM. **(b)** Calibration curve evaluation for the diagnostic potential of the nomogram model. **(c)** Decision curve analysis to assess the practical efficacy of the nomogram.

Analysis of the correlation between biomarkers and the immune microenvironment in GDM

With a clear understanding of the functional background of the biomarkers, a more in-depth analysis was conducted on their impact on the GDM immune microenvironment. Immune infiltration analysis demonstrated that among 28 immune cell types, only eosinophil infiltration scores differed significantly between GDM and control groups, with higher scores observed in the GDM group ($P < 0.05$) (Fig. 5a). Correlation analysis revealed significant positive associations between eosinophil infiltration and MNDA (cor = 0.31, $P = 0.05$), FCGR3B (cor = 0.34, $P = 0.03$), and AQP9 (cor = 0.38, $P = 0.01$) (Fig. 5b-d).

Prediction of the molecular mechanisms of targeted biomarkers

To explore the potential regulatory mechanisms of biomarkers, miRNAs, lncRNAs, TFs, and SNPs targeting the biomarkers were further predicted, and a molecular regulatory network was constructed. Prediction analyses identified four key miRNAs and 122 key lncRNAs (Fig. 6a-b). A lncRNA-miRNA-mRNA regulatory network was constructed, comprising 103 nodes and 126 edges. Within this network, SH3BP5-AS1 was found to regulate AQP9 *via* hsa-miR-182-5p, hsa-miR-154-5p, and hsa-miR-330-3p (Fig. 6c). Additionally, a miRNA-mRNA-TF interaction network with 10 nodes and 9 edges and an SNP-miRNA-mRNA interaction network with 29 nodes and 28 edges were established. Key relationships included hsa-miR-182-5p-AQP9-ELF5, rs765415194-hsa-miR-610-AQP9, and rs771429781-hsa-miR-330-3p-AQP9 (Fig. 6d-e).

Drug prediction for targeted biomarkers

Based on the relatively clear molecular regulatory network of biomarkers, drugs targeting these biomarkers were further predicted, providing new references for targeted therapy for GDM. Drug prediction analyses identified several potential therapeutic agents targeting these biomarkers, including Physostigmine, Glycerin, Urea, Flutamide, Prednisolone, and Alemtuzumab (Fig. 7a-c). Molecular docking revealed hydrogen bond formation between GLN-12 of FCGR3B and Prednisolone (binding energy = -8.9 kcal/mol) and between LYS-77 of MNDA and Physostigmine (binding energy = -6.0 kcal/mol) (Fig. 7d-f, Supplementary Table S1).

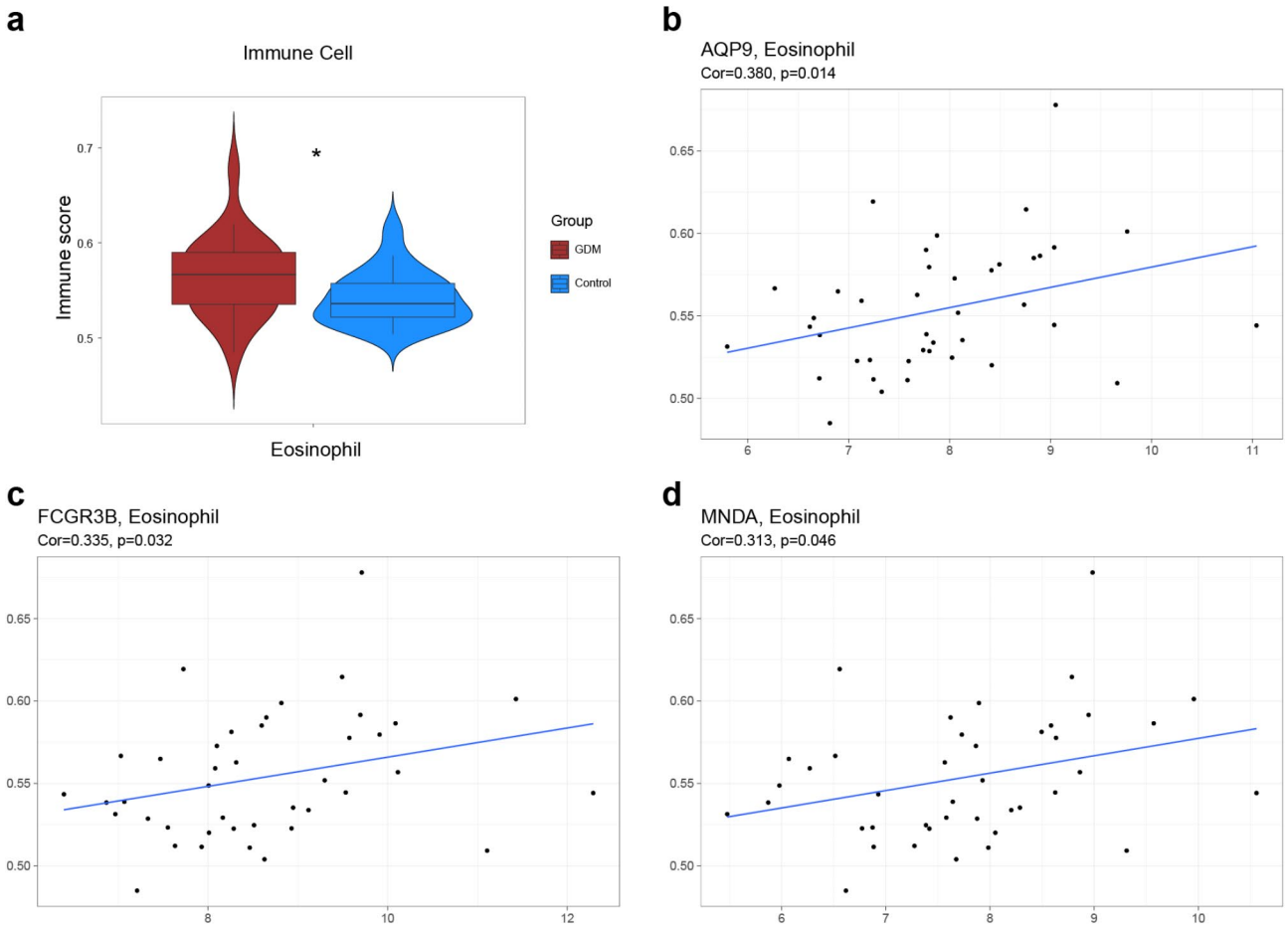

Fig. 5. Relationship of immune cell infiltration with biomarker levels in GDM. **(a)** Immune score of eosinophils between the GDM and control groups (*$P < 0.05$). **(b-d)** Correlation between different biomarkers and eosinophil infiltration: **(b)** AQP9; **(c)** FCGR3B; **(d)** MNDA.

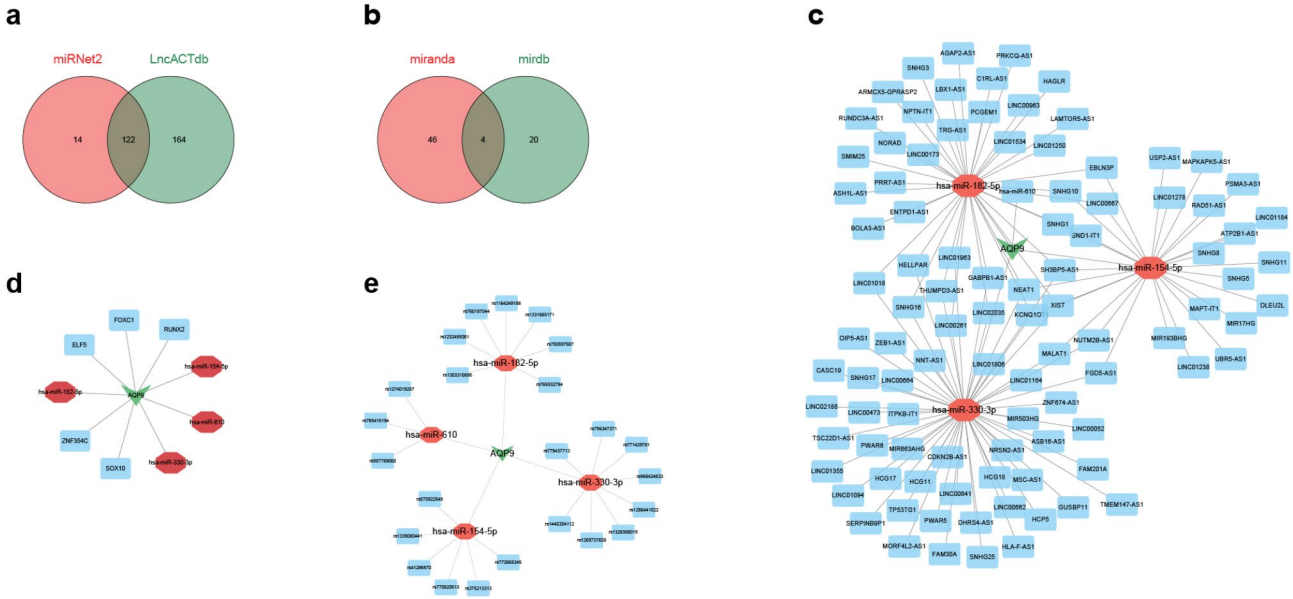

Fig. 6. Molecular regulatory networks of biomarkers. **(a)** Venn diagram of key miRNAs associated with biomarkers. **(b)** Venn diagram of lncRNAs associated with key miRNAs. **(c)** LncRNA-miRNA-mRNA regulatory network of AQP9 (genes in green, miRNAs in red, lncRNAs in blue). **(d)** miRNA-mRNA-TF regulatory network of AQP9 (green for mRNA, red for miRNA, blue for TF). **(e)** SNP-miRNA-mRNA regulatory network of AQP9 (genes in green, miRNAs in red, SNPs in blue). miRNAs, microRNAs; lncRNAs, long non-coding RNAs; TF, transcription factors; SNPs, single nucleotide variants.

Expression evaluation of biomarkers

However, the above analyses were all based on bioinformatics methods. To further investigate the expression levels of the biomarkers in GDM and control samples, RT-qPCR validation was performed on the biomarkers. RT-qPCR analysis evaluated the expression levels of MNDA, FCGR3B, and AQP9 in GDM and control groups (Shapiro-Wilk normality test results was showed in the Supplementary Figure S3). AQP9 exhibited a significant upregulation in the GDM group, consistent with dataset findings ($P = 0.01$). While MNDA ($P = 0.29$) and FCGR3B ($P = 0.70$) showed similar trends to those in the dataset, their differences compared to the control group were not statistically significant (Fig. 8a-c).

Discussion

GDM is a dysglycemic condition resulting from impaired insulin production and resistance during pregnancy, adversely affecting both maternal and offspring health[1,6]. Palmitoylation, a critical lipid modification of membrane-associated proteins, has been implicated in glucose metabolism through multiple pathways[9,10]. Sovio et al. identified a palmitoylated metabolite from maternal serum at 28 weeks of gestational age, named lactosyl-N-palmitoyl-sphingosine, which could strongly and independently predict GDM[13]. Assessing changes in biomarkers of placental tissue will help us understand disease progression, measure treatment effectiveness, and predict future outcomes for pregnant women[20]. However, its precise role in GDM pathogenesis remains unclear.

This study identified and validated three hub palmitoylation-related genes (PRGs)—MNDA, FCGR3B, and AQP9—as potential biomarkers for GDM, proposing them as targets for screening and therapeutic intervention, which would provide important insights into the role of palmitoylation in GDM pathogenesis.

Myeloid nuclear differentiation antigen (MNDA) is a stress-responsive factor predominantly localized in the nucleus of neutrophils and monocytes[21]. It has been recognized as a critical prognostic marker in hematological diseases and certain lymphomas[22]. Abnormal MNDA expression has also been associated with inflammatory disorders, such as systemic lupus erythematosus[23], primary Sjögren's syndrome[24], and chronic obstructive pulmonary disease[25]. A cross-sectional study previously reported elevated expression of MNDA and other inflammation-related genes in myeloid cells of patients with type 1 diabetes (T1D) compared to controls[26]. In this study, MNDA was found to be overexpressed in the placental tissues of patients with GDM relative to controls, as revealed by bioinformatics analysis. These results suggest that MNDA may contribute to GDM progression by modulating inflammatory responses.

Fc-gamma receptors (FCGRs), expressed on immune effector cells, play key roles in immune-mediated diseases. FCGR3B, primarily expressed on neutrophils, is crucial for clearing immune complexes, and its deficiency can prolong inflammation by delaying neutrophil clearance, thereby promoting a proinflammatory state[27,28]. Copy number variations (CNVs) of FCGR3B have been implicated in autoimmune conditions such as systemic lupus erythematosus[29], eosinophilic granulomatosis with polyangiitis[30], and rheumatoid arthritis[31]. Chen et al. identified FCGR3B among ten inflammation-related genes upregulated in GDM placental tissues, contributing to macrophage polarization and placental inflammation[32]. Consistent with these observations, this

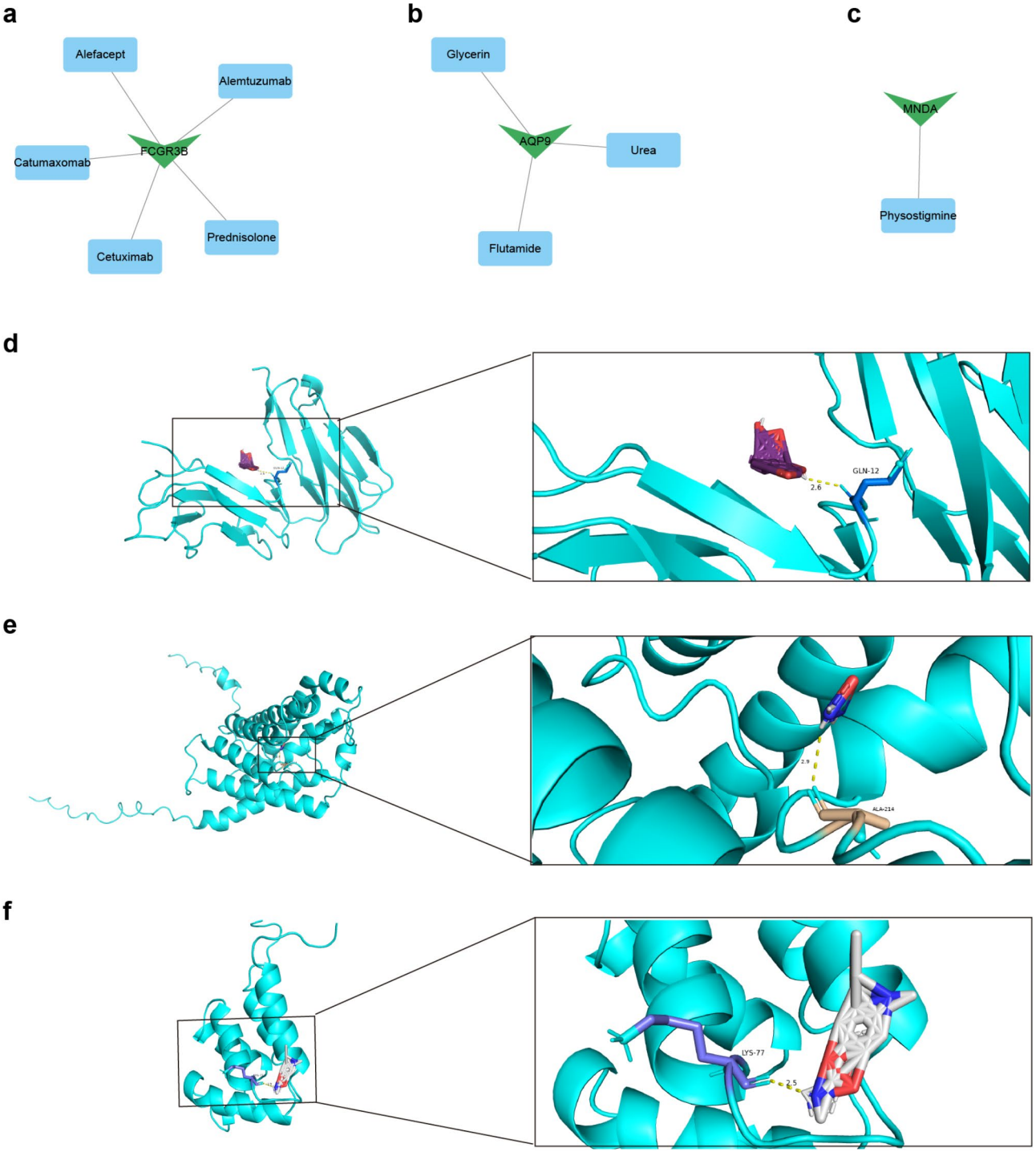

Fig. 7. Drug prediction and molecular docking. **(a-c)** Prediction of biomarker-targeted drugs with potential therapeutic efficacy against GDM: (**a**) FCGR3B-prednisolone, (**b**) AQP9-urea, (**c**) MNDA-physostigmine. **(d-f)** Molecular docking complexes and hydrogen bonds: **(d)** FCGR3B with prednisolone; **(e)** AQP9 with urea; **(f)** MNDA with physostigmine.

study demonstrated that FCGR3B is upregulated in both GDM datasets and clinical samples, underscoring its pivotal role in GDM pathogenesis.

Aquaporins (AQPs) are transmembrane proteins that maintain water homeostasis across cells and tissues. AQP9, predominantly expressed in adipose tissue and liver, regulates blood glucose and energy metabolism by influencing key cellular processes such as gluconeogenesis and fatty acid synthesis[33]. In placental tissue, AQP9 expression exhibits spatial and temporal specificity during pregnancy and has been implicated in pregnancy-related disorders, including preeclampsia and GDM[34,35]. Marino et al. demonstrated that human chorionic

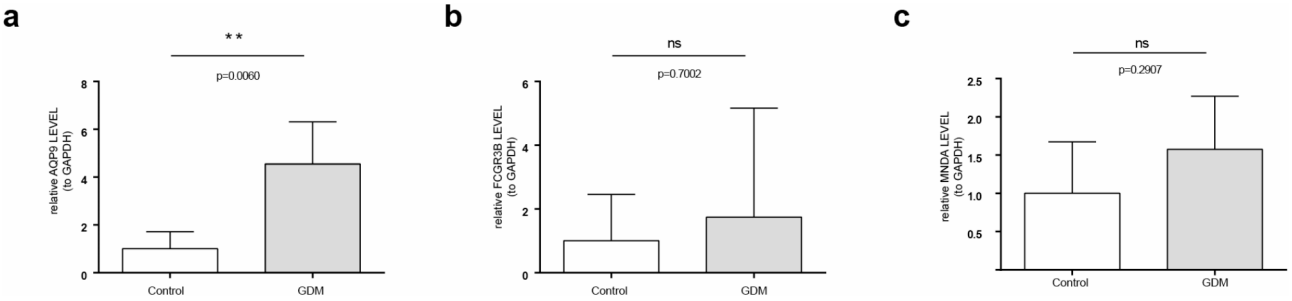

Fig. 8. Expression levels of biomarkers in GDM and control groups. The expression levels of AQP9 (**a**), FCGR3B (**b**), and MNDA (**c**) (**$P<0.01$, ns; $P>0.05$).

gonadotropin increases AQP9 expression *via* cAMP pathways in preeclamptic placentas[36]. Similarly, Pérez-Pérez et al. suggested that the PI3K/Akt/mTOR pathway regulates AQP9 expression in placental cells in response to altered leptin and insulin levels in patients with GDM[37]. This study confirmed the upregulation of AQP9 expression in GDM placental tissues, supported by clinical data, suggesting a significant role for AQP9 in GDM pathogenesis. Although the differences in MNDA and FCGR3B expression between the two group were not clinically verified, both displayed expression trends similar to those observed in the dataset. It is assumed that the relatively small sample size could be a factor contributing to the inconsistency of the results, and further research with larger samples sizes is necessary to confirm our findings.

These genes have been proposed as potential screening and therapeutic targets for GDM. Previous studies investigating the relationship between biomarkers and GDM generally focused on biomarkers from peripheral blood samples taken at different gestational periods, with an emphasis on screening methodologies and diagnostic criteria for GDM. In this study, the nomogram model incorporating MNDA, FCGR3B, and AQP9 demonstrated excellent predictive accuracy and clinical utility, highlighting these PRGs as reliable biomarkers for GDM. However, although the biomarkers are mainly derived from the postpartum placenta, the value of this model in predicting GDM risk is still debatable. Furthermore, the expression of biomarkers may change with the progress and severity of the disease[38,39]. Therefore, differential expression analysis of PRGs in maternal serum at different gestational ages and disease severities may be more effective in predicting GDM. This may be a major part of our future research on the relation between palmitoylation and GDM.

Current research highlights several key pathways involved in GDM pathogenesis, including cell proliferation, metabolism, and inflammatory and immune responses. Ji et al. reported that hyperglycemia in GDM enhances autophagy and apoptosis in placental cells[40]. Moreover, hyperglycemia-induced activation of NLRP3 inflammasomes has been linked to placental inflammation, increasing the risk of metabolic diseases and atherosclerosis in offspring[41]. Elevated serum NLRP3 levels and its effector molecules have been associated with adverse pregnancy outcomes in hyperglycemic women[42]. Animal studies have demonstrated that targeting pathways such as NF-κB/NLRP3 and the NLRP3 inflammasome can mitigate metabolic disorders and organ damage. For instance, tert-butylhydroquinone protects fetal kidneys by reducing oxidative stress and modulating the iNOS/NF-κB/TNF-α signaling pathway[43], while procyanidins improve insulin resistance in GDM mouse models through the NF-κB/NLRP3 pathway[44]. In this study, enrichment analyses revealed that MNDA, FCGR3B, and AQP9 are associated with immune- and inflammation-related pathways, emphasizing their potential as therapeutic targets for managing GDM.

Recent research suggests that GDM represents a state of low-grade inflammation, characterized by altered infiltration, differentiation, and activation of maternal immune cells in placental and visceral adipose tissues[45,46]. In this study, the differences in the infiltration scores of 28 immune cells between the control and GDM groups were compared, and only the eosinophilic infiltration scores were statistically different. However, the precise role of eosinophils in GDM remains unclear. Yuan et al. demonstrated that eosinophils contribute to GDM-associated macrosomia by releasing cytotoxic compounds, such as eosinophil cationic protein encoded by RNASE3[47]. Additionally, galectin-10, a cytoplasmic protein specific to eosinophils and implicated in various eosinophilic disorders, was found to be significantly overexpressed in GDM placentas compared to controls[48]. Consistent with these findings, this study revealed elevated eosinophil infiltration in GDM placentas, with significant positive correlations observed between eosinophil levels and the expression of MNDA, FCGR3B, and AQP9. These results suggest that these three genes may regulate eosinophil function, potentially contributing to the inflammatory pathogenesis of GDM.

Extensive studies highlight the critical regulatory roles of non-coding RNAs (ncRNAs), including microRNAs (miRNAs), long non-coding RNAs (lncRNAs), and circular RNAs, in the development and progression of GDM and its associated complications[49,50]. Sebastiani et al. reported elevated miR-330-3p levels in the plasma of patients with GDM, demonstrating that overexpression of miR-330-3p reduces fasting insulin levels by inhibiting E2F1 and CDC42, key regulators of β-cell growth and proliferation. Notably, the high miR-330-3p subgroup exhibited a higher caesarean section rate compared to the low miR-330-3p subgroup[51]. Conversely, another study found that miR-330-3p expression was significantly elevated in patients with GDM who underwent spontaneous delivery[52]. Weale et al. showed that miR-182-5p is downregulated in T2DM compared to prediabetic individuals[53] and further decreases with disease progression[54]. Although few studies have explored the link between lncRNAs and GDM, some observational studies have revealed distinct expression patterns. For

example, patients with GDM exhibited increased expression of lncRNAs MALAT1 and MEG3, while PVT1 expression was reduced, suggesting their involvement in GDM pathogenesis[55,56]. Additionally, HCP5, a lncRNA highly expressed in GDM, was reported to suppress insulin secretion, with significant implications for long-term metabolic outcomes[57]. LncRNA-associated feedforward loops (lnc-FFLs), formed through interactions among genes, miRNAs, and their shared target lncRNAs[58], have been widely implicated in biological processes and various diseases[59,60]. Fu et al. constructed a global lnc-FFL network, identifying strong associations between hormone-related lnc-FFLs and abnormal glucose metabolism in GDM[61]. SH3BP5-AS1 is a significant lncRNA that has been explored in cancer research but has not been previously evaluated in the context of GDM[62,63].

This study is the first to establish a link between SH3BP5-AS1 and GDM, showing that SH3BP5-AS1 regulates AQP9 through interactions with hsa-miR-182-5p, hsa-miR-154-5p, and hsa-miR-330-3p, which could be a new horizon in investigating the pathogenesis of GDM in terms of palmitoylation. These findings suggest that SH3BP5-AS1 could serve as a novel therapeutic target for GDM. Furthermore, molecular docking and drug prediction analyses identified prednisolone, physostigmine, and urea as potential therapeutic agents for GDM, offering promising avenues for targeted treatment.

Due to the particularity of GDM patients, the therapeutic choices should be more cautious and individualized. Clinically, insulin and metformin were both part of the medication regimen for GDM. Molecular docking is commonly applied in the fields of drug design and screening, leading to the identification of novel therapeutics with improved efficacy, specificity, and safety profiles[64,65]. Sarvesh found that luteolin and naringenin chalcone had strong binding affinities and stable interactions to the target protein AKT1 via molecular docking, suggesting that they may effectively modulate key pathways in GDM[66]. Similarly, we explored drugs targeting these potential biomarkers based on databases. The binding of the drugs to biomarkers was simulated using molecular docking. Our findings present a possible novel therapy for the treatment of GDM patients. As we know, prednisolone is a glucocorticoid used for anti-inflammatory, immunosuppressive, and vasoconstrictive effects clinically. While physostigmine is a reversible acetylcholinesterase inhibitor and widely used in the treatment of glaucoma to reduce intraocular pressure. Urea is used exclusively for the treatment of skin lesions. None of these three drugs are used to treat hypoglycemia. In this study, results of molecular docking and candidate drug analysis indicated that they might be potential candidate agents for the treatment of GDM via palmitoylation-related biomarkers. Our findings present a possible novel therapy for the treatment of GDM patients. The feasibility and efficacy of targeted drugs require further validation through in vitro and in vivo experiments.

Strengths and limitations

In this study, 3 biomarkers (MNDA, FCGR3B and AQP9) significantly related to GDM were successfully identified and their molecular mechanisms were deeply analyzed, providing preliminary evidence for targeting these biomarkers in the treatment of GDM. However, the results may not be representative of the broader population or different subgroups due to limitations in sample size and type. Due to the exploratory nature of this study, the sample size was limited. Despite the application of multiple bioinformatics analysis methods and the exclusion of confounding disease factors, this study has only preliminarily identified differential expression in three genes, with clinical validation failing to fully replicate the bioinformatics findings. Moreover, the investigation was limited by its focus on placentas from patients diagnosed with gestational diabetes mellitus (GDM), which restricted the predictive value for GDM onset. Sovio et al. leveraged data from the Pregnancy Outcome Prediction (POP) study, demonstrating that maternal serum metabolites at 12 and 20 weeks of gestation hold clinical potential for screening and predicting the progression to GDM[13]. Optimal timing for screening (preferably before 20 weeks of gestation) and the selection of appropriate specimens (such as maternal peripheral serum) are thus more clinically significant for GDM prediction. In the future, we will design a larger prospective study to validate the expression of biomarkers at different trimesters of pregnancy, in order to further analyze their potential use as predictive biomarkers for GDM.

Conclusion

This study is the first to identify palmitoylation-associated biomarkers in GDM using bioinformatics analysis, with validation through RT-qPCR. Further exploration highlighted potential pathways involving these biomarkers that may contribute to the etiology of GDM, offering critical insights for identifying effective therapeutic targets. However, additional clinical and experimental research is essential to validate these findings and elucidate the underlying mechanisms. Future investigations will continue to focus on these biomarkers to deepen our understanding of GDM pathogenesis and develop targeted therapeutic strategies.

Methods

Data extraction

GDM-related datasets, namely GSE203346 and GSE154414, were utilized in this study, obtained from the GEO database (http://www.ncbi.nlm.nih.gov/geo/). The GSE203346 dataset, serving as the training set, consisted of placental samples from 21 GDM and 20 control participants, with sequencing performed on the GPL24676 platform. The GSE154414 dataset, sourced from the GPL20301 platform, included placental samples from 4 GDM and 4 control groups. Additionally, 30 PRGs were gathered from published literature, comprising 23 genes involved in palmitoylation and 7 genes associated with de-palmitoylation[10].

Differential expression analysis

To identify genes associated with palmitoylation in GDM, the single-sample gene set enrichment analysis (ssGSEA) algorithm from the GSVA package (v 1.46.0)[67] was used to calculate scores for each sample, using PRGs as the background gene set across all samples in the GSE203346 dataset. Based on the median score,

GDM samples were categorized into high and low-score groups, with comparisons made between the two groups ($P < 0.05$). Furthermore, to further validate the rationality of the grouping between high and low score groups, stratified division was performed using the createFolds function from the caret package (v 6.0–94)[68]. A 5-fold stratified cross-validation was conducted to assess the differences between the high and low score groups ($P < 0.05$). Differential expression analysis was conducted using the DESeq2 package (v 3.4.1)[69] to identify differentially expressed genes (DEGs1) related to palmitoylation in GDM, with a significance threshold of |log2 fold change (FC)| > 0.5 and $P < 0.05$. Similarly, DEGs2 were identified between GDM and control groups within the GSE203346 dataset, using the same analytical approach and significance thresholds. Volcano plots and heatmaps were generated to visualize these DEGs using the ggplot2 (v 3.3.2)[70] and ComplexHeatmap (v 2.14.0)[71] packages.

Characterization of candidate genes

The intersection of DEGs1 and DEGs2 was identified using the ggvenn package (v 0.1.9)[72], highlighting genes associated with both palmitoylation and GDM for further investigation. Spearman correlation analysis, performed using the psych package (v 2.2.9)[73], explored correlations between pairs of intersection genes, with a threshold of |correlation coefficient (cor)| > 0.3 and $P < 0.05$. To investigate the potential biological functions and pathways of the intersection genes, Gene Ontology (GO) biological function annotation and Kyoto Encyclopedia of Genes and Genomes (KEGG) pathway enrichment analyses[74–76] were conducted using the clusterProfiler package (v 4.7.1.003)[77], with $P < 0.05$. GO terms included biological process (BP), cellular component (CC), and molecular function (MF). Additionally, a protein-protein interaction (PPI) network was constructed using the STRING database (https://string-db.org/) with a confidence threshold of > 0.4, and the data were visualized using Cytoscape software (v 3.9.0)[78]. Finally, the intersection genes were further screened using the Degree algorithm from the cytohubba plugin in Cytoscape software. Nodes within the PPI network were ranked according to their degree centrality values, with the top 20 genes selected as candidate genes for subsequent analyses.

Identification of biomarkers

In this study, two machine learning algorithms, randomForest and xgboost, were applied to further screen candidate genes within the GSE203346 dataset. Specifically, the xgboost package (v 1.7.3.1)[79] was utilized to implement the xgboost algorithm, which identified feature genes by assessing their contribution to model accuracy and selecting candidate genes based on the Gini index. Similarly, the randomForest algorithm, executed using the randomForest package (v 4.7.1.1)[80], identified feature genes by evaluating their impact on model accuracy and significance. To refine the selection, intersection analysis of candidate genes based on the top 10 MeanDecreaseAccuracy and MeanDecreaseGini scores further facilitated the identification of feature genes. By overlapping the two sets of feature genes, candidate biomarkers were obtained. The expression of these candidate biomarkers between the GDM and control groups in both the GSE203346 and GSE154414 datasets was compared using the Wilcoxon test. Candidate biomarkers that demonstrated consistent expression patterns across both datasets and significant differences between the groups ($P < 0.05$) were designated as palmitoylation-associated biomarkers in GDM.

Distribution of biomarkers

In order to further investigate the biological functions of biomarkers, analyze the interactions between genes, and understand their roles in cellular functions, chromosome mapping analysis of the biomarkers was conducted. To visualize the chromosomal location of these biomarkers, the RCircos package (v 1.2.2)[81] was employed. Subsequently, through tissue expression, the expression patterns of different biomarkers in tissues were further analyzed. Biomarker information was imported into the biology gene portal services (BioGPS) (http://biogps.org) to obtain data on their distribution across relevant tissues. The tissue distribution data for each biomarker were then imported into Cytoscape software to construct a network map, illustrating the relationships between tissues and biomarkers, with the top 10 tissues/organs exhibiting the highest gene expression selected for the map. Finally, through subcellular localization analysis, the specific location of biomarkers within the cell was determined, which helped to understand the localization characteristics of different biomarkers and further analyze their distinct roles within the cell. For subcellular distribution information, the biomarkers were imported into the Genecards database (https://www.genecards.org/), with subcellular distribution data selected at a confidence level of 5, and used to generate network maps depicting associations between subcellular locations and biomarkers in Cytoscape.

Development and validation of the nomogram

To predict the likelihood of GDM development based on the biomarkers, a nomogram was constructed using the rms package (v 6.7.1)[82] in the GSE203346 dataset. Biomarker expression levels in the samples were scored, and the sum of these scores represented the total points, which were used to predict the probability of GDM. A higher total score corresponded to a higher likelihood of developing GDM. The accuracy and applicability of the nomogram model were evaluated using calibration curves and decision curves, which were generated with the PredictABEL (v 1.2.4)[83] and ggDCA (v 1.2)[84] packages, respectively, further validating the model's predictive power.

Functional and annotation analyses

The biomarker enrichment scores for each sample in the GSE203346 dataset were calculated using the ssGSEA algorithm from the GSVA package, based on the expression matrix of biomarkers in both the GDM and control groups. Samples were then classified into high and low expression groups according to the median enrichment score. Differences in significant enrichment pathways between the two groups were compared using the limma

package (v 3.42.2)[85], with significance defined as $P < 0.05$ and $|t| > 2$. The background gene set used for the analysis was "c2.cp.kegg.v2023.1.Hs.symbols.gmt" from the Molecular Signatures Database (MSigDB) (http://software.broadinstitute.org/gsea/msigdb).

The clusterProfiler package was used to perform Gene Set Enrichment Analysis (GSEA) in the GSE203346 dataset to identify signaling pathways associated with biomarkers in GDM. Spearman correlation analysis was conducted using the psych package to examine the relationships between biomarkers and all genes in the dataset, followed by sorting of genes based on their correlation coefficients. The background gene set for GSEA was selected from MSigDB, specifically "h.all.v2022.1.Hs.entrez.gmt." Multiple test correction was applied using the Benjamini and Hochberg methods to adjust *P*-values. The screening criteria for significance were set at P.adjust < 0.05, false discovery rate (FDR) < 0.25, and |normalized enrichment score (NES)| > 1. Visualization of results was conducted using the enrichplot package (v 1.18.3)[86].

Immune infiltration analysis

To assess immune cell infiltration, 28 immune cell profiles[87] were obtained from the TISIDB (an integrated repository portal for tumor-immune system interactions) database (http://cis.hku.hk/TISIDB/). These data were analyzed using the ssGSEA algorithm in the GSVA package. The differences in infiltration scores of the 28 immune cells between the high and low expression groups were compared using the Wilcoxon test ($P < 0.05$). Additionally, Spearman's correlation analysis was employed to examine the relationships between differential immune cell infiltration and the biomarkers, with a correlation coefficient threshold of $|cor| > 0.3$ and $P < 0.05$.

Establishment of molecular regulatory networks

Molecular regulatory networks were constructed to further investigate the mechanisms underlying biomarkers. Initially, miRNAs associated with biomarkers were identified using the miranda (http://www.microrna.org/microrna/home.do) and miRDB (http://mirdb.org/) databases through the multiMiR package (v 1.20.0)[88]. The miRNAs predicted by both databases were intersected to obtain key miRNAs. Next, upstream regulators, specifically long non-coding RNAs (lncRNAs) of these key miRNAs, were predicted using the LncACTdb (http://bio-bigdata.hrbmu.edu.cn/LncACTdb) and miRNet (https://www.mirnet.ca/miRNet/home.xhtml) databases. The predicted lncRNAs from both databases were then intersected to identify key lncRNAs. Consequently, a lncRNA-miRNA-mRNA regulatory network, comprising biomarkers, key miRNAs, and key lncRNAs, was constructed.

The NetworkAnalyst website (https://www.networkanalyst.ca) was employed to analyze miRNA databases and predict interactions between miRNAs and biomarkers using the TargetScan (https://www.targetscan.org/vert_80/) and miRDB databases. Interactions between biomarkers and transcription factors (TFs) were predicted based on the JASPAR database (https://jaspar.elixir.no/). The resulting prediction data were imported into Cytoscape software for visualization of the miRNA-mRNA-TF network.

To explore the association between single nucleotide variants (SNPs) and biomarkers, the miRNASNP-v3 database (https://guolab.wchscu.cn/miRNASNP/) was used to predict SNPs in the miRNA seed region, based on the miRNAs incorporated into the miRNA-mRNA-TF network. This analysis aimed to clarify how SNPs within the miRNA seed region influence their binding to the 3' UTR region of biomarkers. A curated list of SNP-miRNA-mRNA combinations was subsequently generated by selecting relevant biomarkers. Finally, an interaction network encompassing these relationships was constructed.

Drug prediction and molecular Docking analyses

To identify potential small-molecule drugs for GDM therapy, biomarkers were queried in the Genecards database (https://www.genecards.org/) to explore approved drugs with potential therapeutic efficacy against GDM. One drug for each biomarker, predicted to be a potential therapeutic, was selected for molecular docking to examine the protein-drug interaction patterns. Two-dimensional molecular structural formulas of the drugs were obtained from the PubChem database (https://pubchem.ncbi.nml.gov), while key protein structures were retrieved from the Protein Data Bank (PDB) database (https://www.rcsb.org/). Molecular docking was performed using AutoDock Vina (v 1.2.2)[89], and the resulting conformations with the lowest binding energies and capable of forming hydrogen bonds were visualized using PyMol (v 3.3.0)[90]. Docking scores below − 5 kcal/mol were considered indicative of strong binding affinity between compound-target pairs, and complexes that established critical hydrogen bonds were expected to demonstrate enhanced biological activity.

Reverse transcription-quantitative polymerase chain reaction (RT-qPCR)

To further validate the results of the public database analysis, five GDM placental tissue samples were collected from The Third Affiliated Hospital of Zhengzhou University, with control placental samples obtained from five healthy individuals (Supplementary Table S2). The study excluded pregnant women with asthma, smokers, and those with other maternal or fetal conditions, including hypertension, preeclampsia, and placenta praevia. These tissue samples were used for RT-qPCR analysis. The study received approval from the Medical Ethics Committee of The Third Affiliated Hospital of Zhengzhou University (approval code: 2023-239-01), and informed consent was obtained from all patients. Total RNA from the 10 samples was isolated using TRIzol (Ambion, Austin, USA) following the manufacturer's instructions. Total RNA was reverse transcribed into cDNA using the SureScript First-strand cDNA synthesis kit (Servicebio, Wuhan, China) as per the manufacturer's guidelines. qPCR was performed using the 2x Universal Blue SYBR Green qPCR Master Mix (Servicebio, Wuhan, China), and primers used for PCR are listed in Supplementary Table S3. Notably, the Shapiro-Wilk normality test was used to further analyze whether the data followed a normal distribution ($p > 0.05$, indicating normal distribution), and a Q-Q plot was generated to visualize the results. Expression levels were normalized to GAPDH and calculated using the $2^{-\Delta\Delta Ct}$ method[91].

Statistical analysis

Data analysis was performed using R software (v 4.2.2), with the Wilcoxon test used to assess differences between groups. A *P*-value of less than 0.05 was considered statistically significant.

Data availability

The datasets analysed during the current study are available in the [GEO] repository, [http://www.ncbi.nlm.nih.gov/geo/, GSE203346/GSE154414]; [Genecards database] repository, [https://www.genecards.org/]; [PubChem database] repository, [https://pubchem.ncbi.nml.gov] and [Protein Data Bank (PBD) database]repository, [https://www.rcsb.org/]

Received: 27 October 2024; Accepted: 4 March 2025
Published online: 07 March 2025

References

1. McIntyre, H. D. et al. Gestational diabetes mellitus. *Nat. Reviews Disease Primers*. **5** https://doi.org/10.1038/s41572-019-0098-8 (2019).
2. White, S. L., Ayman, G., Bakhai, C., Hillier, T. A. & Magee, L. A. Screening and diagnosis of gestational diabetes. *Bmj* https://doi.org/10.1136/bmj-2022-071920 (2023).
3. Davidson, K. W. et al. Screening for gestational diabetes: US preventive services task force recommendation statement. *Jama-journal Am. Med. Association*. **326**, 531–538 (2021).
4. Sweeting, A. et al. Epidemiology and management of gestational diabetes. *Lancet* **404**, 175–192 (2024).
5. Wahlberg, J. et al. Gestational diabetes: glycaemic predictors for fetal macrosomia and maternal risk of future diabetes. *Diabetes Res. Clin. Pract.* **114**, 99–105. https://doi.org/10.1016/j.diabres.2015.12.017 (2016).
6. Ye, W. et al. Gestational diabetes mellitus and adverse pregnancy outcomes: systematic review and meta-analysis. *Bmj* **377**, e067946. https://doi.org/10.1136/bmj-2021-067946 (2022).
7. Chamberlain, L. H. & Shipston, M. J. The physiology of protein S-acylation. *Physiol. Rev.* **95**, 341–376. https://doi.org/10.1152/physrev.00032.2014 (2015).
8. F, S. M. et al. Mechanisms and functions of protein S-acylation. *Nat. Rev. Mol. Cell Biol.* **25**, 488–509. https://doi.org/10.1038/s41580-024-00700-8 (2024).
9. Niu, J. et al. Fatty acids and cancer-amplified ZDHHC19 promote STAT3 activation through S-palmitoylation. *Nature* **573**, 139–143 (2019).
10. Kong, Y. et al. Palmitoylation landscapes across human cancers reveal a role of palmitoylation in tumorigenesis. *J. Translational Med.* **21**, 826 (2023).
11. Dong, G. et al. Palmitoylation couples insulin hypersecretion with B cell failure in diabetes. *Cell Metabol.* **35**, 332–344. .e337 (2023).
12. Du, K., Murakami, S., Sun, Y., Kilpatrick, C. L. & Luscher, B. DHHC7 palmitoylates glucose transporter 4 (Glut4) and regulates Glut4 membrane translocation. *J. Biol. Chem.* **292**, 2979–2991. https://doi.org/10.1074/jbc.M116.747139 (2017).
13. Sovio, U. et al. Metabolomic identification of a novel, externally validated predictive test for gestational diabetes mellitus. *J. Clin. Endocrinol. Metabolism*. **107**, e3479–e3486 (2022).
14. Khaire, A. A., Thakar, S. R., Wagh, G. N. & Joshi, S. R. Placental lipid metabolism in preeclampsia. *J. Hypertens.* **39**, 127–134 (2021).
15. Yong, H. E. J. et al. Increasing maternal age associates with lower placental CPT1B mRNA expression and acylcarnitines, particularly in overweight women. *Front. Physiol.* **14**, 1166827 (2023).
16. Melini, S. et al. Co-Micronized palmitoylethanolamide and Rutin associated with Hydroxytyrosol recover Diabesity-Induced hepatic dysfunction in mice: in vitro insights into the synergistic effect. *Phytother. Res.* **38**, 6035–6047 (2024).
17. Wang, M. et al. Astragaloside IV protects renal tubular epithelial cells against oxidative stress-induced injury by upregulating CPT1A-mediated HSD17B10 lysine succinylation in diabetic kidney disease. *Phytother. Res.* **38**, 4519–4540 (2024).
18. Qu, M., Zhao, Y., Qing, X., Zhang, X. & Li, H. Androgen-dependent miR-125a-5p targets LYPLA1 and regulates global protein palmitoylation level in late-onset hypogonadism males. *J. Cell. Physiol.* **236**, 4738–4749 (2021).
19. Wild, A. R. et al. Exploring the expression patterns of palmitoylating and de-palmitoylating enzymes in the mouse brain using the curated RNA-seq database BrainPalmSeq. *eLife* 11, null (2022).
20. Wang, W. J. et al. Genome-Wide placental gene methylations in gestational diabetes mellitus, fetal growth and metabolic health biomarkers in cord blood. *Front. Endocrinol.* **13**, 875180 (2022).
21. Bottardi, S. et al. MNDA, a PYHIN factor involved in transcriptional regulation and apoptosis control in leukocytes. *Front. Immunol.* **15**, 1395035 (2024).
22. Bellos, F. et al. Myeloid nuclear differentiation antigen (MNDA) expression: A useful marker in the diagnosis of myelodysplastic syndromes by flow cytometry. *Blood* **126**, 5235–5235 (2015).
23. Liu, C. et al. Identification of crucial genes for predicting the risk of atherosclerosis with system lupus erythematosus based on comprehensive bioinformatics analysis and machine learning. *Comput. Biol. Med.* **152**, 106388 (2023).
24. Hou, Q. et al. Bioinformatics analyses of potentially common pathogenic networks for primary Sjögren's syndrome complicated with acute myocardial infarction. *Sci. Rep.* **13**, 19276 (2023).
25. Esteve-Codina, A. et al. Gender specific airway gene expression in COPD sub-phenotypes supports a role of mitochondria and of different types of leukocytes. *Sci. Rep.* **11**, 12848 (2021).
26. Jin, Y. et al. The expression of inflammatory genes is upregulated in peripheral blood of patients with type 1 diabetes. *Diabetes Care*. **36**, 2794–2802 (2013).
27. Willcocks, L. C. et al. Copy number of FCGR3B, which is associated with systemic lupus erythematosus, correlates with protein expression and immune complex uptake. *J. Exp. Med.* **205**, 1573–1582 (2008).
28. Zaghlool, S. B. et al. Epigenetics Meets proteomics in an epigenome-wide association study with Circulating blood plasma protein traits. *Nat. Commun.* **11**, 15 (2020).
29. McKinney, C. & Merriman, T. R. Meta-analysis confirms a role for deletion in FCGR3B in autoimmune phenotypes. *Hum. Mol. Genet.* **21**, 2370–2376 (2012).
30. Martorana, D. et al. Fcγ-receptor 3B (FCGR3B) copy number variations in patients with eosinophilic granulomatosis with polyangiitis. *J. Allergy Clin. Immunol.* **137**, 1597–1599e1598 (2016).
31. Ben Kilani, M. S., Cornélis, F., Olaso, R., Chaudru, V. & Petit-Teixeira, E. Investigation of candidate gene copy number identifies FCGR3B as a potential biomarker for rheumatoid arthritis. *Clin. Exp. Rheumatol.* **37**, 923–928 (2019).
32. Chen, C., Yang, Z. & Qiu, Z. Bioinformatics prediction and experimental validation of the role of macrophage polarization and ferroptosis in gestational diabetes mellitus. *J. Inflamm. Res.* **16**, 6087–6105. https://doi.org/10.2147/jir.S440826 (2023).
33. Maeda, N. Implications of Aquaglyceroporins 7 and 9 in glycerol metabolism and metabolic syndrome. *Mol. Aspects Med.* **33**, 665–675 (2012).

34. Bednar, A. D., Beardall, M. K., Brace, R. A. & Cheung, C. Y. Differential expression and regional distribution of aquaporins in amnion of normal and gestational diabetic pregnancies. *Physiological reports* 3, null (2015).
35. Pérez-Pérez, A. et al. Aquaporins and placenta. *Vitam. Horm.* **112**, 311–326 (2020).
36. Marino, G. I., Castro-Parodi, M., Dietrich, V. & Damiano, A. E. High levels of human chorionic gonadotropin (hCG) correlate with increased aquaporin-9 (AQP9) expression in explants from human preeclamptic placenta. *Reproductive Sci.* **17**, 444–453 (2010).
37. Vilariño-García, T. et al. Increased expression of Aquaporin 9 in trophoblast from gestational diabetic patients. *Hormone Metabolic Res. = Hormon- Und Stoffwechselforschung = Horm. Et Metab.* **48**, 535–539. https://doi.org/10.1055/s-0042-105152 (2016).
38. Dias, S., Pheiffer, C., Abrahams, Y., Rheeder, P. & Adam, S. Molecular Biomarkers for Gestational Diabetes Mellitus. *International journal of molecular sciences* 19, null (2018).
39. Zhang, Z., Zhou, Z. & Li, H. The role of lipid dysregulation in gestational diabetes mellitus: early prediction and postpartum prognosis. *J. Diabetes Invest.* **15**, 15–25 (2024).
40. Ji, L. et al. Systematic characterization of autophagy in gestational diabetes mellitus. *Endocrinology* **158**, 2522–2532 (2017).
41. Govindarajah, V. et al. Gestational diabetes in mice induces hematopoietic memory that affects the long-term health of the offspring. *Journal of clinical investigation* 134, null (2024).
42. Han, N. et al. Relationship between serum NLRP3 along with its effector molecules and pregnancy outcomes in women with hyperglycemia. *J. Maternal-Fetal Neonatal Med.* **37**, 2312447 (2024).
43. Li, J., Liu, H. & Shang, L. Tert-butylhydroquinone mitigates renal dysfunction in pregnant diabetic rats via Attenuation of oxidative stress and modulation of the iNOs/ NFkB/TNF alpha signalling pathway. *Endocr. Metabolic Immune Disorders-Drug Targets.* **23**, 633–646 (2023).
44. Liu, Y. et al. Procyanidins and its metabolites by gut Microbiome improves insulin resistance in gestational diabetes mellitus mice model via regulating NF-κB and NLRP3 inflammasome pathway. *Biomed. Pharmacother.* **151**, 113078 (2022).
45. Katzman, P. J. Chronic inflammatory lesions of the placenta. *Semin. Perinatol.* **39**, 20–26 (2015).
46. McElwain, C. J., McCarthy, F. P. & McCarthy, C. M. Gestational Diabetes Mellitus and Maternal Immune Dysregulation: What We Know So Far. *International journal of molecular sciences* 22, null (2021).
47. Yuan, Y., Zhu, Q., Yao, X., Shi, Z. & Wen, J. Maternal Circulating metabolic biomarkers and their prediction performance for gestational diabetes mellitus related macrosomia. *BMC Pregnancy Childbirth*. **23**, 113 (2023).
48. Buschmann, C. et al. Galectin-10 expression in placentas of women with gestational diabetes. *Curr. Issues. Mol. Biol.* **45**, 8840–8851 (2023).
49. Filardi, T. et al. Non-Coding RNA: Role in Gestational Diabetes Pathophysiology and Complications. *International journal of molecular sciences* 21, null (2020).
50. Zhang, T. N., Wang, W., Huang, X. M. & Gao, S. Y. Non-Coding RNAs and extracellular vehicles: their role in the pathogenesis of gestational diabetes mellitus. *Front. Endocrinol.* **12**, 664287 (2021).
51. Sebastiani, G. et al. Circulating MicroRNA (miRNA) expression profiling in plasma of patients with gestational diabetes mellitus reveals upregulation of MiRNA miR-330-3p. *Front. Endocrinol.* **8**, 345 (2017).
52. Pfeiffer, S. et al. Circulating miR-330-3p in late pregnancy is associated with pregnancy outcomes among lean women with GDM. *Sci. Rep.* **10**, 908 (2020).
53. Weale, C. J. et al. Circulating miR-30a-5p and miR-182-5p in prediabetes and Screen-Detected diabetes mellitus. *Diabetes Metabolic Syndrome Obesity: Targets Therapy.* **13**, 5037–5047 (2020).
54. Weale, C. J. et al. Expression profiles of Circulating MicroRNAs in South African type 2 diabetic individuals on treatment. *Front. Genet.* **12**, 702410 (2021).
55. Lu, J., Wu, J., Zhao, Z., Wang, J. & Chen, Z. Circulating LncRNA serve as fingerprint for gestational diabetes mellitus associated with risk of macrosomia. *Cell. Physiol. Biochem.* **48**, 1012–1018 (2018).
56. Tang, L., Li, P. & Li, L. Whole transcriptome expression profiles in placenta samples from women with gestational diabetes mellitus. *J. Diabetes Invest.* **11**, 1307–1317 (2020).
57. Zhao, H., Zhan, J., Wang, Q., Yang, S. & Xiao, X. LncRNA HCP5 is highly expressed in gestational diabetes mellitus to suppress insulin secretion. *Diabetes Metabolic Syndrome Obesity: Targets Therapy.* **17**, 157–163 (2024).
58. Zhang, H. M. et al. Transcription factor and MicroRNA co-regulatory loops: important regulatory motifs in biological processes and diseases. *Brief. Bioinform.* **16**, 45–58 (2015).
59. Jiang, L. et al. Identification of transcription factor-miRNA-lncRNA feed-forward loops in breast cancer subtypes. *Comput. Biol. Chem.* **78**, 1–7 (2019).
60. Yan, Z. et al. Integrative analysis of gene and MiRNA expression profiles with transcription factor-miRNA feed-forward loops identifies regulators in human cancers. *Nucleic Acids Res.* **40**, e135 (2012).
61. Fu, X. et al. Construction of Glycometabolism- and Hormone-Related lncRNA-Mediated feedforward loop networks reveals global patterns of LncRNAs and drug repurposing in gestational diabetes. *Front. Endocrinol.* **11**, 93 (2020).
62. Zhao, X., Zhu, X., Xiao, C. & Hu, Z. LncRNA SH3BP5-AS1 promotes hepatocellular carcinoma progression by sponging miR-6838-5p and activation of PTPN4. *Aging* **16**, 8511–8523 (2024).
63. Lin, C. et al. N6-methyladenosine-mediated SH3BP5-AS1 upregulation promotes GEM chemoresistance in pancreatic cancer by activating the Wnt signaling pathway. *Biol. Direct*. **17**, 33 (2022).
64. García-Ortegón, M. et al. Easy molecular Docking yields better benchmarks for ligand design. *J. Chem. Inf. Model.* **62**, 3486–3502 (2022).
65. Wu, K., Karapetyan, E., Schloss, J., Vadgama, J. & Wu, Y. Advancements in small molecule drug design: A structural perspective. *Drug Discovery Today*. **28**, 103730 (2023).
66. Sabarathinam, S., Jayaraman, A. & Venkatachalapathy, R. Gut Microbiome-Derived Metabolites and Their Impact on Gene Regulatory Networks in Gestational Diabetes. *Journal of steroid biochemistry and molecular biology* null, 106674 (2025).
67. Hänzelmann, S., Castelo, R. & Guinney, J. GSVA: gene set variation analysis for microarray and RNA-seq data. *BMC Bioinform.* **14**, 7 (2013).
68. Zeng, P. et al. Association of metabolic syndrome severity with frailty progression among Chinese middle and old-aged adults: a longitudinal study. *Cardiovasc. Diabetol.* **23**, 302 (2024).
69. Love, M. I., Huber, W. & Anders, S. Moderated Estimation of fold change and dispersion for RNA-seq data with DESeq2. *Genome Biol.* **15**, 550 (2014).
70. Gustavsson, E. K., Zhang, D., Reynolds, R. H., Garcia-Ruiz, S. & Ryten, M. Ggtranscript: an R package for the visualization and interpretation of transcript isoforms using ggplot2. *Bioinformatics* **38**, 3844–3846 (2022).
71. Gu, Z., Eils, R. & Schlesner, M. Complex heatmaps reveal patterns and correlations in multidimensional genomic data. *Bioinformatics* **32**, 2847–2849 (2016).
72. Mao, W., Ding, J., Li, Y., Huang, R. & Wang, B. Inhibition of cell survival and invasion by Tanshinone IIA via FTH1: A key therapeutic target and biomarker in head and neck squamous cell carcinoma. *Experimental Therapeutic Med.* **24**, 521 (2022).
73. Robles-Jimenez, L. E. et al. Worldwide Traceability of Antibiotic Residues from Livestock in Wastewater and Soil: A Systematic Review. *Animals: an open access journal from MDPI* 12, null (2021).
74. Kanehisa, M. Toward Understanding the origin and evolution of cellular organisms. *Protein Sci.* **28**, 1947–1951 (2019).
75. Kanehisa, M., Furumichi, M., Sato, Y. & Kawashima, M. Ishiguro-Watanabe, M. KEGG for taxonomy-based analysis of pathways and genomes. *Nucleic Acids Res.* **51**, D587–d592 (2023).
76. Kanehisa, M. & Goto, S. KEGG: Kyoto encyclopedia of genes and genomes. *Nucleic Acids Res.* **28**, 27–30 (2000).

77. Wu, T. et al. ClusterProfiler 4.0: A universal enrichment tool for interpreting omics data. *Innov. (New York N Y)*. **2**, 100141 (2021).
78. Shannon, P. et al. Cytoscape: a software environment for integrated models of biomolecular interaction networks. *Genome Res.* **13**, 2498–2504 (2003).
79. Hou, N. et al. Predicting 30-days mortality for MIMIC-III patients with sepsis-3: a machine learning approach using XGboost. *J. Translational Med.* **18**, 462 (2020).
80. Alderden, J. et al. Predicting pressure injury in critical care patients: A Machine-Learning model. *Am. J. Crit. Care.* **27**, 461–468 (2018).
81. Zhang, H., Meltzer, P. & Davis, S. RCircos: an R package for circos 2D track plots. *BMC Bioinform.* **14**, 244 (2013).
82. Xu, J. et al. A nomogram for predicting prognosis of patients with cervical cerclage. *Heliyon* **9**, e21147 (2023).
83. Kundu, S., Aulchenko, Y. S., van Duijn, C. M. & Janssens, A. C. PredictABEL: an R package for the assessment of risk prediction models. *Eur. J. Epidemiol.* **26**, 261–264 (2011).
84. Luo, Y. et al. RNA modification gene WDR4 facilitates tumor progression and immunotherapy resistance in breast cancer. *Journal of Advanced Research* null, null (2024).
85. Ritchie, M. E. et al. Limma powers differential expression analyses for RNA-sequencing and microarray studies. *Nucleic Acids Res.* **43**, e47 (2015).
86. Wang, L. et al. Cuproptosis related genes associated with Jab1 shapes tumor microenvironment and Pharmacological profile in nasopharyngeal carcinoma. *Front. Immunol.* **13**, 989286 (2022).
87. Charoentong, P. et al. Pan-cancer Immunogenomic analyses reveal Genotype-Immunophenotype relationships and predictors of response to checkpoint Blockade. *Cell. Rep.* **18**, 248–262 (2017).
88. Ru, Y. et al. The MultiMiR R package and database: integration of microRNA-target interactions along with their disease and drug associations. *Nucleic Acids Res.* **42**, e133 (2014).
89. Trott, O. & Olson, A. J. AutoDock Vina: improving the speed and accuracy of Docking with a new scoring function, efficient optimization, and multithreading. *J. Comput. Chem.* **31**, 455–461 (2010).
90. Seeliger, D. & de Groot, B. L. Ligand Docking and binding site analysis with PyMOL and Autodock/Vina. *J. Comput. Aided Mol. Des.* **24**, 417–422 (2010).
91. Shang, Y. et al. Decreased E2F2 expression correlates with poor prognosis and immune infiltrates in patients with colorectal Cancer. *J. Cancer.* **13**, 653–668 (2022).

Acknowledgements

We would like to express our sincere gratitude to all individuals and organizations who supported and assisted us throughout this research. Special thanks to the Medical Science and Technology Project of Health Commission of Henan Province.

Author contributions

Z.K. Conceptualization. Z.K. and B.R.R. Investigation. Z.K. and S.X.Y. Methodology. Z.K. and S.X.Y. Project administration. Z.K. Writing-original draft. R.C.C. Supervision. Y.L. and R.C.C. Writing-review and editing. All authors reviewed and agreed to the published version of the manuscript.

Funding

This work was supported by Henan Provincial Medical Science and Technology Project (2018020204) and Henan Provincial Medical Science and Technology Project (LHGJ20190614).

Declarations

Competing interests

The authors declare no competing interests.

Ethics declarations

The study was conducted in strict accordance with the principles outlined in the World Medical Association Declaration of Helsinki. This study was approved by the Medical Ethics Committee of The Third Affiliated Hospital of Zhengzhou University(approval code: 2023-239-01), and written informed consent was obtained from each patient.

Additional information

Supplementary Information The online version contains supplementary material available at https://doi.org/10.1038/s41598-025-93046-w.

Correspondence and requests for materials should be addressed to C.R.